ELSEVIER

Journal of Molecular Structure (Theochem) 632 (2003) 227–234

THEO CHEM

www.elsevier.com/locate/theochem

An averaged solvent electrostatic potential/molecular dynamics study of the influence of the electron correlation on the properties of liquid hydrogen fluoride

A. Muñoz Losa, I. Fdez. Galván, M.E. Martín, M.A. Aguilar*

Departamento de Química Física, Universidad de Extremadura, Avda de Elvas, s/n 06071 Badajoz, Spain

Received 4 November 2002; accepted 23 December 2002

Abstract

We study the influence that the choice of the electron correlation calculation method has on the thermodynamic, electrical, and structural properties of liquid hydrogen fluoride (HF) as obtained by Quantum Mechanics/Molecular Mechanics methods (QM/MM). We consider also the influence of the basis set and Lennard–Jones parameters. In our study we applied a non-traditional QM/MM method that makes use of the mean field approximation. We found that the influence of the correlation and basis set can be easily understood in terms of the values in the gas phase of the dipole moment and polarizabilities that they lead to. The main factor that determines the vaporization energy is the in vacuo dipole moment.

Keywords: Liquid hydrogen fluoride; Quantum mechanics/Molecular mechanics methods; Lennard–Jones Parameters

1. Introduction

Quantum Mechanics/Molecular Mechanics (QM/MM) methods [1–3] are now widely employed in the study of molecules in solution. The main advantage of these methods is that they combine a quantum description of part of the system, permitting chemical processes to be studied, with a detailed description of the solvent obtained from simulation techniques. In most QM/MM methods we have to solve the solute Schrödinger equation for each solvent configuration, which means several thousand quantum calculations. As a consequence most calculations published to date have been performed at a semi-empirical [1], Hartree-Fock self-consistent field [2] (HF-SCF), or density functional theory [3] (DFT) level, and using reduced basis sets.

In previous papers [4] we have developed a non-traditional QM/MM method that makes use of the mean field approximation [5] (MFA). In this approximation, the average value of the energies of the different solute–solvent configurations is replaced by the energy of the average configuration. Our method is based on the calculation from the simulation data of the Averaged Solvent Electrostatic Potential (ASEP). The ASEP is then introduced into the molecular Hamiltonian of the solute. This approximation, named ASEP/MD, reduces drastically the number of quantum calculations (from several thousand to only

* Corresponding author. Fax: +34-9-24-275576.
E-mail address: maguilar@unex.es (M.A. Aguilar).

0166-1280/03/$ - see front matter © 2003 Elsevier B.V. All rights reserved.
doi:10.1016/S0166-1280(03)00301-4

a few), and introduces no significant inaccuracies. This reduced number of quantum calculations permits us to study questions not approachable by traditional QM/MM methods.

Our main aim in this paper is to study the influence that the choice of the basis set and the electron correlation calculation method have on the thermodynamic, electrical, and structural properties of the liquid. We pay special attention to the consideration of the electron correlation, which is calculated by using very different methods: second order Moeller–Plesset perturbation theory (MP2), the multiconfigurational self-consistent field method (MCSCF), and DFT. We include both perturbation and variational methods.

As a case study we chose hydrogen fluoride (HF) in its liquid phase. This liquid has been studied both theoretically [6–15] and experimentally [16,17]. The image that one has is of an associated liquid with strong hydrogen bonds, where the molecules undergo strong polarization with respect to the in vacuo situation. These characteristics make liquid HF a severe test for any theory of the liquid state.

The outline of the paper is as follows. In Section 2 the details of the ASEP/MD method are described. In Sections 3–5, the influence of the basis set, electron correlation, and Lennard–Jones parameters on the thermodynamics and structure of the liquid are analyzed. Lastly, in Section 6 some conclusions are drawn.

2. Details of the computational scheme

The ASEP/MD method for the study of liquids and solutions has been described in detail in a number of publications [4]. As in traditional QM/MM methods [1–3], in ASEP/MD the energy and state function of the solvated solute molecule are obtained by solving the effective Schrödinger equation:

$$(\hat{H}_{\mathrm{QM}} + \hat{H}_{\mathrm{QM-MM}})|\Psi\rangle = E|\Psi\rangle \tag{1}$$

The interaction term, $\hat{H}_{\mathrm{QM/MM}}$ takes the following form:

$$\hat{H}_{\mathrm{QM/MM}} = H^{\mathrm{elect}}_{\mathrm{QM/MM}} + H^{\mathrm{vdw}}_{\mathrm{QM/MM}} \tag{2}$$

$$\hat{H}^{\mathrm{elect}}_{\mathrm{QM/MM}} = \int \mathrm{d}r\cdot\hat{\rho}\cdot\langle\hat{V}_{\mathrm{S}}(r;\rho)\rangle \tag{3}$$

where $\hat{\rho}$ is the solute charge density and the brackets denote a statistical average. The term $\langle\hat{V}_{\mathrm{S}}(r;\rho)\rangle$ is the averaged electrostatic potential generated by the solvent at the position r, and is obtained from MD calculations where the solute molecule is represented by the charge distribution ρ supposed fixed during the simulation. The term $\hat{H}^{\mathrm{vdw}}_{\mathrm{QM/MM}}$ is the Hamiltonian for the van der Waals interaction, in general represented by a Lennard–Jones (LJ) potential. Given that the solvent structure, and hence the ASEP, is a function of the solute charge density, Eqs. (1) and (3) have to be solved iteratively. In general only a few cycles of quantum calculation/molecular dynamics simulations are needed for convergence. The procedure is shown in Fig. 1. If, as is the case for pure liquids, the solute and solvent molecules are the same then the solute charge distribution obtained from the quantum calculation also allows the charge distribution of the solvent molecules to be updated, i.e. all the molecules are simultaneously polarized. The ASEP/MD is thus half-way between a non-polarizable simulation (the MD is performed at fixed values of the charges) and a polarizable simulation (the charge distribution is updated at each cycle of the procedure).

All quantum calculations were performed with the program Gaussian 98 [18]. Four types of basis sets

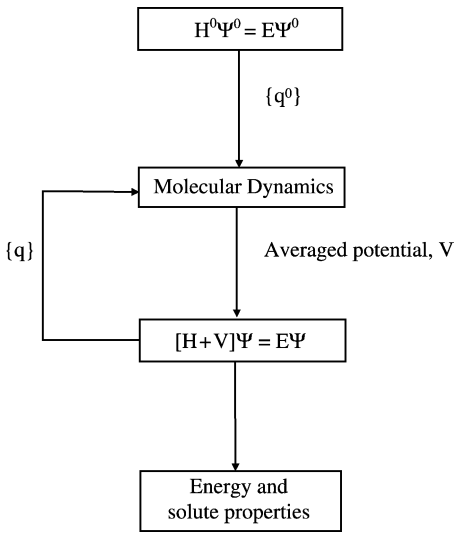

Fig. 1. Flow chart of the coupled ASEP/MD model.

were used: 6-31 G* [19a–d], 6-311G** [19e,f], aug-cc-pVDZ [20a] and aug-cc-pVTZ [20b] hereafter referred as B1, B2, B3 and B4, respectively. Four different levels of calculation were used:

(a) Hartree-Fock Self-consistent field method (HF-SCF).
(b) Density functional theory (DFT), using the density-gradient-corrected correlation functional proposed by Perdew [21] and Becke's [22] exchange functional.
(c) Moeller–Plesset perturbation theory at second order (MP2), considering two variants. In the first, MP2(E), the corrections are applied when the ASEP/MD cycle has finished and only to the HF-SCF energy, i.e. the solute charge distribution is that obtained at the HF-SCF level. In the second, MP2, at each step of the ASEP/MD cycle both the energy and the state function are obtained with the MP2 method.
(d) Multiconfigurational Self-Consistent Field (MCSCF) method, using the HF-SCF orbitals as starting orbitals in the subsequent CASSCF calculations. The complete active space was spanned by all the configurations arising from eight valence electrons in seven orbitals. Individually optimized state functions were used.

The MD calculations were performed using the program MOLDY [23]. A total of 216 molecules were simulated at fixed intramolecular geometry by combining Lennard–Jones interatomic interactions with electrostatic interactions in a cubic simulation box of 19.19 Å side. The geometry was the gas phase experimental value [24] ($d_{H-F} = 0.917$ Å). The HF molecules were represented during the simulation through two point charges placed on the hydrogen and fluorine atoms. These charges were obtained by fitting the molecular electrostatic potential of the solute molecule polarized by the solvent. Previous studies [9,10,12] have shown that, for an adequate description of the zig-zag structure of the hydrogen bond chain in the liquid, a representation based on the use of a three-site potential works better. We will remove this deficiency in future work. In this paper we focus more on analyzing the effect of the basis set and electron correlation than on getting perfect agreement with the experimental data. The Lennard–Jones potential parameters were taken from Cournoyer and Jorgensen [10] (CJ). In a few cases expressly indicated these parameters were changed to study their influence on the liquid's properties. Periodic boundary conditions were applied, and spherical cut-offs were used to truncate the molecular interactions at 9.0 Å. A time step of 0.5 fs was used. The electrostatic interaction was calculated with the Ewald method. The temperature was fixed at 278 K using a Nosé-Hoover [25] thermostat. Each MD calculation simulation was run for 150,000 timesteps (50,000 equilibration, 100,000 production).

In order to facilitate subsequent discussion, we give in Table 1 the in vacuo dipole moments and polarizabilities obtained with different basis sets and methods.

3. Thermodynamic results

Table 2 lists for comparison the vaporization energies and their components calculated at several levels and with different basis sets. Prior to the discussion of the results it is necessary to clarify the meaning of the different terms that appear in the table. For a pure liquid the vaporization energies can be calculated as

$$\langle E \rangle = \tfrac{1}{2}(E_{elect} + E_{vdw}) + E_{dist} \quad (4)$$

where E_{elect} is the QM/MM electrostatic solute–solvent interaction energy that includes the interaction with the polarized charges. The electrostatic interaction energy is hence the sum of two contributions, one due to interaction between the permanent charges, $E_{elect,perm}$, and the other to the interaction between the induced charges, $E_{elect,ind}$. The first contribution,

Table 1
In vacuo dipole moments and polarizabilities calculated with several basis sets and methods

	HF-SCF				DFT	MCSCF	Exp.
	B1	B2	B3	B4	B3	B3	
μ^0 (debye)	1.98	2.02	1.93	1.93	1.73	1.74	1.82[a]
α^0 (Å^3)	0.26	0.39	0.66	0.71	0.74	0.73	0.83[b]

[a] Ref. [29].
[b] Ref. [12].

Table 2
Influence of the basis set on the vaporization energy and its components (in kcal /mol)

	HF-SCF				
	B1	B2	B3	B4	Exp.
E_{vap}	−7.3	−7.3	−6.3	−6.5	−6.9[a]
E_{elect}	−21.7	−21.9	−20.5	−20.7	
$E_{elect,perm}$	−13.0	−13.5	−10.2	−10.2	
$E_{elect,ind}$	−8.7	−8.4	−10.3	−10.5	
E_{LJ}	3.3	3.5	3.5	3.3	
E_{dist}	1.9	1.9	2.2	2.2	
μ (debye)	2.38	2.42	2.42	2.41	
$\Delta\mu$ (debye)	0.40	0.41	0.49	0.48	

Values obtained at the HF-SCF level.
[a] Ref. [30].

$E_{elect,perm}$, is calculated in the first ASEP/MD cycle, before the solute polarization begins, and all the molecules are represented by their in vacuo charges. $E_{elect,ind}$ is calculated as the difference between the total electrostatic interaction energy and the permanent electrostatic contribution. E_{vdw} is the solute–solvent Lennard–Jones interaction energy and E_{dist} is the distortion energy of the solute, i.e. the energy spent in polarizing one HF molecule. This energy is calculated as the difference:

$$E_{dist} = \langle \Psi | H^0 | \Psi \rangle - \langle \Psi^0 | H^0 | \Psi^0 \rangle \quad (5)$$

where Ψ and Ψ^0 are the in solution and in vacuo state functions, respectively.

The vaporization energies, Table 2, calculated at HF-SCF level are in good accord with the experimental data, the errors being 5.8, 5.8, −8.7, and −5.8% for the basis sets B1, B2, B3 and B4, respectively. (The minus sign means that the energy is underestimated.) The main factor that determines the value of the vaporization energy seems to be the value of the in vacuo dipole moment. Thus, the largest vaporization energies are obtained with B1 and B2, which are the basis sets that provide the highest values of the in vacuo dipole moment and the lowest polarizabilities. As expected, these basis sets yield the highest value of $E_{elect,perm}$ and the lowest value of $E_{elect,ind}$. When we use larger basis sets, B3 and B4, the increase in the induction energy does not compensate the decrease in $E_{elect,perm}$ and the final result is a decrease in the vaporization energy. This trend, larger contribution of the permanent charges and smaller of the induced charges when we decrease the basis set size, has been described previously in QM/MM simulations of water [26]. Furthermore, the basis sets B1 and B2 provide the lowest values of the induced dipole moments and hence of the distortion energies.

For the four basis sets considered, the largest contribution to the vaporization energy comes from the electrostatic component. For the larger basis sets, this component splits almost equally between $E_{elect,perm}$ and $E_{elect,ind}$. In B1 and B2, however, the permanent charge contribution predominates. In principle, and given that the four basis sets yield values very close to the in solution dipole moment, one would expect the same value for E_{elect}. However, differences of about 1.2 kcal/mol are found. These differences are mainly due to the contribution of higher multipole moments of the solute (note that the solute is treated quantum-mechanically and hence it includes automatically all the multipole contributions). The sum of the contributions of the quadrupole multipole and higher terms works in opposition to the dipole contribution: it decreases the absolute value of the vaporization energy, and, for instance, is lower with the basis B2 (+1 kcal/mol) than with B3 (+1.8 kcal/mol).

The inclusion of the electron correlation, see Table 3, decreases the value of E_{vap} by about 1.2–1.5 kcal/mol. However, the origin of this decrease is different according to which calculation method is used. In the variational methods, DFT and MCSCF, all the components of the energy decrease. These two methods provide the lowest in vacuo dipole moment and hence the lowest values of $E_{elect,perm}$. Due

Table 3
Vaporization energies and their components (in kcal/mol) calculated with different methods and the B3 basis set

	HF-SCF	MP2(E)	MP2	DFT	MCSCF	Exp.
E_{vap}	−6.3	−5.1	−4.9	−4.8	−4.9	−6.9
E_{elect}	−20.5	−20.5	−19.2	−13.4	−13.3	
$E_{elect,perm}$	−10.2	−10.2	−10.2	−6.5	−6.5	
$E_{elect,ind}$	−10.3	−10.3	−9.0	−6.9	−6.8	
E_{LJ}	3.5	3.5	3.0	1.2	1.2	
E_{dist}	2.2	3.4	3.2	1.3	1.2	
μ (debye)	2.42	2.42	2.40	2.15	2.12	
$\Delta\mu$ (debye)	0.49	0.49	0.47	0.42	0.38	

to the low value of the in vacuo dipole moment the reaction field is low and the solvent is less structured (see below), and as a consequence the three components of the interaction energy decrease. On the contrary, in the perturbation method MP2 the electrostatic and Lennard–Jones components are very similar to the HF-SCF value. In this case the decrease in the vaporization energy is mainly related to the increase of the distortion energy. It is interesting to note that MP2(E), which is the simplest and most economical correlated method to apply recovers almost all the change in the vaporization energy. For the four methods considered, the largest contribution to the vaporization energy comes from the electrostatic component that splits almost equally between $E_{\text{elect,perm}}$ and $E_{\text{elect,ind}}$.

Table 4 gives the results obtained with different sets of LJ parameters. In addition to the CJ parameters we used the set proposed by Jedlovszky and Vallaury [13] (JVp) developed for use with polarizable potentials. The vaporization energy is very sensitive to the use of different LJ parameters. The JVp set yields too low a vaporization energy, a fact related to the use of too high a value of the van der Waals radii. Table 4 also lists the results obtained when the van der Waals radius is modified in a systematic way. Taking as reference the CJ set, we decreased the van der Waals radius by 0.03 and 0.08 Å. The electrostatic component decreases with the radius, but the vaporization energy displays a non-linear behavior: it passes through a minimum. In principle when we decrease the van der Waals radius the absolute value of the vaporization energy should increase. However, if we continue decreasing the radius then, although the electrostatic interaction increases, so does the distortion and LJ energies which are both repulsive. The increase of these two components compensates the increase of the electrostatic component and results in a decrease of the vaporization energy.

Table 4
Influence of the LJ parameters on the vaporization energies and their components (in kcal/mol)

	CJ	CJ1	CJ2	JVp
E_{vap}	−6.3	−7.5	−7.1	−5.2
E_{elect}	−20.5	−25.8	−28.7	−11.8
E_{LJ}	3.5	4.5	6.4	−0.1
E_{dist}	2.2	3.1	4.0	0.7
μ(D)	2.41	2.49	2.55	2.21
Δμ(D)	0.48	0.56	0.62	0.28

Energies calculated at the HF-SCF level with the B3 basis set. CJ stands for the Cournoyer and Jorgensen parameters ($\varepsilon = 0.6020$ kcal/mol, $\sigma = 2.98$ Å); CJ1 corresponds to $\varepsilon = 0.6020$ kcal/mol, $\sigma = 2.95$ Å; CJ2 to $\varepsilon = 0.6020$ kcal/mol, $\sigma = 2.90$ Å; and JVp are the Jedlovszky and Vallaury parameters ($\varepsilon = 0.8745$ kcal/mol, $\sigma = 3.05$ Å).

4. Polarization

In this section we consider the influence that the solvent has on the charge distribution of the HF molecule. The bottom two rows of Tables 2–4 list the values of the total and induced dipole moments. The total in solution dipole moment varies between 2.12 and 2.42 debye depending on the basis set and correlation method used. The variations are smaller in the induced dipole moment, between 0.38 and 0.49 debye. In any case, it is clear that the solution produces a notable increase in the dipole moment.

The smallest variations in the induced dipole correspond to the methods DFT and CASCF, and this is so despite these two methods yielding the largest value of the polarizability. In principle, and given that in an approximate way $\Delta\mu = \alpha E$, where α is the polarizability and E is the electric field felt by the molecule, one might think that the principal factor that determines the value of the induced dipole moment would be the polarizability. However, the electric field is a function of the structure of the solvent around the solute and this is mainly determined by the electrostatic solute–solvent interactions, and hence, as we have shown before, by the value of the in vacuo dipole moment, which is lower in the DFT and MCSCF methods.

At the HF-SCF level the four basis sets considered yield similar values of the electrostatic component and of the in vacuo dipole moment (and, as we will see below, a very similar structure of the solvent). In this case the final value of the induced dipole moment is correlated with the polarizability.

For the in solution dipole moment, Tables 3 and 4, there are no experimental values available, and we compare our results with that obtained by Jedlovszky and Vallaury using a polarizable potential. These authors get an induced dipole moment of 0.51 debye.

This value compares very well with our results, especially those provided by the B3 and B4 basis sets. Our model, however, yields the largest values of the in solution dipole moment when it is calculated at the RHF level. Thus, Jedlovszky and Vallaury obtain 2.23 debye while our values are close to 2.4 debye. This difference is in part due to the overestimate of the in vacuo dipole moment and in part to the overestimate of the solvent structure around the solute. At the DFT and MCSCF levels, the agreement with the JV-p result is almost complete both in the induced and in the total dipole moments.

Table 4 list the induced dipole moments obtained with different LJ parameters. The JVp parameters underestimate the induced dipole moment, which now is only 0.28 debye. This result is coherent with the low value of the electrostatic component of the solute–solvent interaction energy that these parameters give. When the LJ parameters were systematically varied we found that the induced dipole moment decreases with the van der Waals radius.

5. Structural results

For comparison with the experimental results [16,17] we produced an intermolecular rdf by adding the FF, HF and HH rdfs together. We followed the procedure proposed by Pfleiderer et al. [17] so that, in the simulation, the total $g(r)$ was calculated as a weighted average of the three partial pair correlation functions:

$$g(r) = 0.210 g_{FF}(r) + 0.497 g_{HF}(r) + 0.293 g_{HH}(r) \quad (6)$$

The four basis sets yield very similar radial distribution functions. There are only minimal differences in the heights of the peaks. For this reason we display only the B4 results. Compared with the experimental curve, Fig. 2, the peaks obtained at the HF-SCF level are well placed, at 1.65, 2.55 and 3.35 Å. The experimental curve shows two peaks at 1.62 Å and 2.53–2.56 Å and a broad peak centered around 3.30–3.38 Å. However, the HF-SCF curve has more peaks than the experimental curve at large distances and the height of the peaks is clearly overestimated, and this is so even though the vaporization energy given by the HF-SCF method agreed very well with the experimental value. This overestimate of the solvent structure around the solute is related to two factors: first, to the use of a two-site model for the HF molecule during the simulation, and second, to the use of the MFA. In a previous paper [27] we have shown that this approximation yields a rdf where the height of the peaks is slightly overestimated when compared with the results

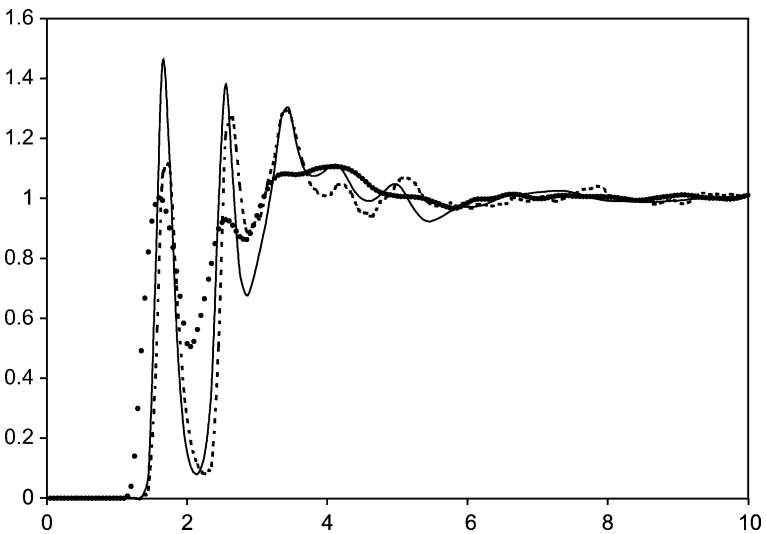

Fig. 2. Comparison of the total pair correlation function of HF as obtained from neutron diffraction experiments [17] (dots), and calculated at HF-SCF (solid line) and MP2 (dashed line) levels.

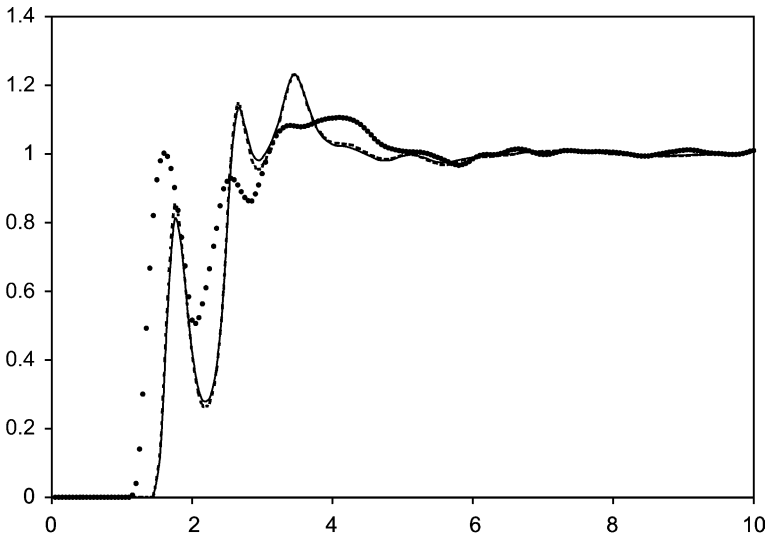

Fig. 3. Comparison of the total pair correlation function of HF as obtained from neutron diffraction experiments [17] (dots), and calculated at DFT (dashed line) and MCSCF (solid line) levels.

obtained by other QM/MM methods [28] that do not use the MFA.

The inclusion of the electron correlation, Fig. 3, at the CASSCF or DFT levels, modifies this image. The height of the peaks decreases, in parallel with the decrease of the vaporization energy and the in vacuo dipole moment, and the peak position is shifted out to greater distances. In general the agreement with the experimental curve is worse. On the contrary, when the MP2 method is used the results improve. MP2 yields rdfs that are very similar to those obtained at the HF-SCF level. The peaks are well placed and the height of the first peak decreases and fits better the experimental result. The heights of the second and third peaks are overestimated.

6. Conclusions

We have applied a QM/MM method that makes use of the MFA to study liquid HF. The HF-SCF calculations yielded vaporization energies that agreed well with the experimental value, and a rdf where the peaks are in the correct place but where the heights are overestimated. Furthermore, the in solution dipole moment compares well with the values proposed by JVp using a polarizable potential. We analyzed the influence that the choice of the basis set and of the consideration of the electron correlation has on the picture of the liquid. This influence can be understood in terms of the in vacuo dipole moment and polarizability values. The final value of the vaporization energy is mainly determined by the value of the in vacuo dipole moment. The behavior of the induced dipole moment is somewhat more complex. In this case, there are influences of both the polarizability and the in vacuo dipole moment. The solvent structure is mainly a function of the electrostatic interaction component, which in turn is a function of the value of the in vacuo dipole moment.

The inclusion of electron correlation always decreases the vaporization energy. However, the origin of this decrease is different depending on the nature of the method. In the variational methods, DFT and MCSCF, it is related to the decrease in the in vacuo dipole moment. On the contrary, in the perturbation methods, MP2, the decrease in the vaporization energy is mainly related to the increase of the distortion energy. Of the methods studied, MP2 yielded values of the induced dipole moments and rdf functions that best agreed with the experimental values and with the values obtained by other authors.

Acknowledgements

This research was sponsored by the Dirección General de Investigación Científica y Técnica (Project no. BQU2000-0243) and by the Consejería de Educación Ciencia y Tecnología de la Junta de Extremadura (Project no 2PR01A010).

References

[1] A. Warshel, M. Levitt, J. Mol. Biol. 103 (1976) 227. M.J. Field, P.A. Bash, M. Karplus, J. Comput. Chem. 11 (1990) 700. V. Luzhkov, A. Warshel, J. Comput. Chem. 13 (1992) 199. J. Gao, J. Phys. Chem. 96 (1992) 537. V.V. Vasilyev, A.A. Bliznyuk, A.A. Voityuk, Int. J. Quantum Chem. 44 (1992) 897. V. Théry, D. Rinaldi, J.L. Rivail, B. Maigret, G.G. Ferenczy, J.Comput. Chem. 15 (1994) 269. M.A. Thompson, E.D. Glendening, D. Feller, J. Phys. Chem. 98 (1994) 10465.

[2] N. Vaidehi, T.A. Wesolowski, A. Warshel, J. Chem. Phys. 97 (1992) 4264. R.V. Stanton, L.R. Little, K.M. Merz, J. Phys. Chem. 99 (1995) 17344. N.W. Moriarty, G. Karlström, J. Phys. Chem. 100 (1996) 17791. Y. Tu, A. Laaksonen, J. Chem. Phys. 111 (1999) 7519.

[3] D. Wei, D.R. Salahub, Chem. Phys. Lett. 224 (1994) 291. I. Tuñón, M.T.C. Martins-Costa, C. Millot, M.F. Ruiz-López, J.L. Rivail, J. Comput. Chem. 17 (1996) 19. T.A. Wesolowski, A. Warshel, J. Phys. Chem. 97 (1993) 8050. T.A. Wesolowski, A. Warshel, J. Phys. Chem. 98 (1994) 5183. T.A. Wesolowski, R.P. Muller, A. Warshel, J. Phys. Chem. 100 (1996) 15444.

[4] M.L. Sánchez, M.A. Aguilar, F.J. Olivares del Valle, J. Comput. Chem. 18 (1997) 313. M.L. Sánchez, M.E. Martín, M.A. Aguilar, F.J. Olivares del Valle, Chem. Phys. Lett. 310 (1999) 195. M.E. Martín, M.L. Sánchez, J. Olivares del Valle, M.A. Aguilar, J. Chem. Phys. 113 (2000) 6308. M.E. Martín, M.L. Sánchez, M.A. Aguilar, F.J. Olivares del Valle, J. Mol. Struct. (Theochem) 537 (2001) 213. M.L. Sánchez, M.E. Martín, M.A. Aguilar, F.J. Olivares del Valle, J. Comput. Chem. 21 (2000) 705. M.E. Martín, M.L. Sánchez, F.J. Olivares del Valle, M.A. Aguilar, J. Chem. Phys. 116 (2002) 1613.

[5] M.L. Sánchez, M.E. Martín, I. Fdez-Galván, F.J. Olivares del Valle, M.A. Aguilar, J. Phys. Chem. 106 (2002) 4813.

[6] M.L. Klein, I.R. McDonald, S.F. O'Shea, J. Chem. Phys. 69 (1978) 63.

[7] W.L. Jorgensen, M.E. Cournoyer, J. Am. Chem. Soc. 100 (1978) 4942.

[8] W.L. Jorgensen, J. Chem. Phys. 70 (1979) 5888.

[9] M.L. Klein, I.R. McDonald, J. Chem. Phys. 71 (1979) 298.

[10] M.E. Cournoyer, W. Jorgensen, Mol. Phys. 51 (1984) 119.

[11] U. Röthlisberger, M. Parrinello, J. Chem. Phys. 106 (1997) 4658.

[12] P. Jedlovszky, R. Vallauri, Mol. Phys. 92 (1997) 331.

[13] P. Jedlovszky, R. Vallauri, J. Chem. Phys. 107 (1997) 10166.

[14] R.G. Della Valle, D. Gazzillo, Phys. Rev. B 59 (1999) 13699.

[15] P. Jedlovszky, M. Mezei, R. Vallauri, J. Chem. Phys. 115 (2001) 9883.

[16] M. Deraman, J.C. Dore, J.G. Powles, J.H. Holloway, P. Chieux, Mol. Phys. 55 (1985) 1351.

[17] T. Pfleiderer, I. Waldner, H. Bertagnolli, K. Tödheide, H.E. Fischer, J. Chem. Phys. 113 (2000) 3690.

[18] M.J. Frisch, G.W. Trucks, H.B. Schlegel, G.E. Scuseria, M.A. Robb, J.R. Cheeseman, V.G. Zakrzewski, J.A. Montgomery Jr., R.E. Stratmann, J.C. Burant, S. Dapprich, J.M. Millam, A.D. Daniels, K.N. Kudin, M.C. Strain, O. Farkas, J. Tomasi, V. Barone, M. Cossi, R. Cammi, B. Mennucci, C. Pomelli, C. Adamo, S. Clifford, J. Ochterski, G.A. Petersson, P.Y. Ayala, Q. Cui, K. Morokuma, D.K. Malick, A.D. Rabuck, K. Raghavachari, J.B. Foresman, J. Cioslowski, J.V. Ortiz, A.G. Baboul, B.B. Stefanov, G. Liu, A. Liashenko, P. Piskorz, I. Komaromi, R. Gomperts, R.L. Martin, D.J. Fox, T. Keith, M.A. Al-Laham, C.Y. Peng, A. Nanayakkara, C. Gonzalez, M. Challacombe, P.M.W. Gill, B. Johnson, W. Chen, M.W. Wong, J.L. Andres, C. Gonzalez, M. Head-Gordon, E.S. Replogle, J.A. Pople, Gaussian 98, Gaussian, Inc., Pittsburgh, PA, 1998.

[19] (a) R. Ditchfield, W.J. Hehre, J.A. Pople, J. Chem. Phys. 54 (1971) 724. (b) W.J. Hehre, R. Ditchfield, J.A. Pople, J. Chem. Phys. 56 (1972) 2257. (c) P.C. Hariharan, J.A. Pople, Mol. Phys. 27 (1974) 209. (d) M.S. Gordon, Chem. Phys. Lett. 76 (1980) 163. (e) A.D. McLean, G.S. Chandler, J. Chem. Phys. 72 (1980) 650. (f) R. Krishnan, J.S. Binkley, R. Seeger, J.A. Pople, J. Chem. Phys. 72 (1980) 650.

[20] (a) D.E. Woon, T.H. Dunning Jr., J. Chem. Phys. 98 (1993) 1358. (b) R.A. Kendall, T.H. Dunning Jr., R.J. Harrison, J. Chem. Phys. 96 (1992) 6796.

[21] J. Perdew, Phys. Rev. B 33 (1986) 8822.

[22] A.D. Becke, J. Chem. Phys. 98 (1993) 5648.

[23] K. Refson, Moldy User's Manual Rev. 2.10, University of Oxford, Oxford, 1996, ftp.earth.ox.ac.uk/pub

[24] M. Kofranek, H. Lishka, A. Karpfen, Chem. Phys. 121 (1988) 137.

[25] W.G. Hoover, Phys. Rev. A 31 (1985) 1695.

[26] G. Jansen, F. Colonna, J.G. Ángyán, Int. J. Quantum Chemistry 58 (1996) 251.

[27] M.E. Martín, M.A. Aguilar, S. Chalmet, M.F. Ruiz López, Chem. Phys. Letter 344 (2001) 107.

[28] I. Tuñon, M.T.C. Martins-Costa, C. Millot, M.F. Ruiz López, J. Mol. Model. 1 (1995) 196. I. Tuñon, M.T.C. Martins-Costa, C. Millot, M.F. Ruiz López, J. Chem. Phys. 106 (1997) 3633. S. Chalmet, M.F. Ruiz-López, J. Chem. Phys. 111 (1999) 1117.

[29] J.S. Muentner, W. Klemperer, J. Chem. Phys. 52 (1970) 6033. C.G. Gray, K.E. Gubbins, Theory of Molecular Fluids, vol. 1, FundamentalsClarendon PressOxford (1984) pp. 579; Appendix D.

[30] C.E. Vanderzee, W.W. Rodenburg, J. Chem. Thermodyn. 2 (1970) 461.